

The Influence of Electrophoretic Deposition (EPD) Parameters on SS430 Spinel Coated Characteristic

Yohannes Nyambong Lowrance¹, Mohd Azham Azmi^{1*}, Lufti Mohd Basar¹, Hamimah Abd Rahman¹

¹Faculty of Mechanical and Manufacturing Engineering,
Universiti Tun Hussein Onn Malaysia, Batu Pahat, 86400, MALAYSIA

*Corresponding Author

DOI: <https://doi.org/10.30880/ijie.2021.13.02.030>

Received 26 December 2019; Accepted 13 December 2020; Available online 28 February 2021

Abstract: The interconnect that is applied with protective coating which is $(\text{MnCO})_3\text{O}_4$ spinel coated stainless steel is crucial to enhance solid oxide fuel cell (SOFC) performance. In this research, commercial manganese cobalt $(\text{MnCO})_3\text{O}_4$ is used by electrophoretic deposition (EPD) method as a protective layer on ferritic stainless steel. Elemental energy dispersive X-ray spectroscopy (EDS) was examined for the spinel coated interconnect $(\text{MnCO})_3\text{O}_4$. Scanning Electron Microscope (SEM) examines the surface morphology and coating thickness. The EPD $(\text{MnCO})_3\text{O}_4$ spinel coated interconnect is carried out with 30V to 50V with duration of coating from 20s in an aqueous suspension. The best covering parameter can be determined by observing the deposition morphology and density of the EPD at 40V and 45V for 20s. This article examines the impact of voltage deposition. The objectives of these study is to obtain the best parameter for the interconnect coating while experimenting with the voltage. 78.8 μm with even and thick surface coating is the maximum deposition thickness achieved. Voltage deposition can therefore be concluded to affect the efficiency of the electrical conductivity of steel.

Keywords: $(\text{MnCO})_3\text{O}_4$, solid oxide fuel cell (SOFC), electrophoretic deposition (EPD), elemental energy dispersive X-ray spectroscopy (EDS)

1. Introduction

Due to its ability to generate electrical energy through chemical reaction without combustion and mechanical processes, Solid oxide fuel cell (SOFC) has created a spark in research, making it a green energy [1]–[3]. SOFC consists of three major components, cathode, anode and electrolyte. The fuel cell can operate at around 600°C to 1000°C at high temperatures to allow electrochemical reactions to occur. Most SOFC application needs to be developed in stacks to meet the power requirements of the application operation. The SOFC is connected via interconnects to operate. Interconnects conduct electricity between the cell and separate the combustion of fuel and gas oxide [4].

Electricity conductivity and excellent heat expansions behaviour, while low price, are commonly applied as interconnections [5]–[8]. Nevertheless, the use of Cr-containing stainless steel has two primary drawbacks. The chromium evaporation induced by water vapor response and also the gradual oxidation decreases the efficiency of steel interconnections [9]–[12]. Ceramic coatings, particularly perovskite and spinel type, are commonly used in surface protection, but the low thermochemical stability of perovskite ceramics due to the diffusion of chrome cations is difficult. [6], [13], [14]. Spinel coatings with comparatively excellent conductivity, by comparison, have a low migration rate of Cr. The layer of the spinel is usually produced by means of sol-gel dip [15], slurry coating [14], aerosol deposition [6] and electrophoretic deposition (EPD) [8]. In this case, EPD is the most suitable spinel coating

*Corresponding author: azham@uthm.edu.my

technique used for stainless steel interconnect. EPD offers simple control of the thickness and morphology of the deposited coating through basic change of the deposition time and applied deposition voltage [16].

EPD is a colloidal method in which a ceramic structure consists directly of a stable electric DC colloid suspension. [17]. The deposition electrode is in the form of the necessary goods and facilitates the release of the deposit. DC is used for moving charge particles to and from the opposite loading electrode [18]. EPD is a mixture of two procedures of electrophoresis in which the movement of loaded particles in suspension under the impact of the electrical field and the deposition in which the coagulation of particles occurs at a thick mass [11].

There are a number of variables that should be considered for the incorporation of EPD coating techniques which are the suspension stability, the correlation of pH scales and the interaction between particles in the suspension and the mechanism of EPD and the kinetics of electrophoretic deposition [19]. In this study, deposition voltage plays a huge role in determining the suitable parameters for spinel coated SS430 type stainless steel. The deposition voltage used are 30V, 35V, 40V, 45V, 50V with deposition time of 20s. The EPD testing included in this study are the SEM which includes surface morphology, the coating thickness and the EDS, the area specific resistance (ASR) *via* NOVA 1.11 Autolab for 100 hour. Through this, a study on the effect of voltage deposition will be discussed in this paper.

2. Materials and Method

2.1 Material selection

A commercial $(\text{MnCO})_3\text{O}_4$ was used for protective coatings for which the steel interconnect or substrate used are SS430. The steel substrates are cutted into 1.5×2 mm² sizes and are polish by using sand paper before cleaning it in acetone bath by ultrasonic for 30 minutes with temperature of 50°C.

2.2 Electrophoretic Deposition

Suspension of 400ml are prepared which consists of 50% ethanol (200ml), 50% deionized water (200ml) and also 4 g of $(\text{MnCO})_3\text{O}_4$. Suspension ratio is 1000 ml: 10g. The suspension are kept at a constant pH of 5 it provides the suitable stability for the suspension. The suspension is sonicated until the suspension is homogenous and there are no sediments below the beaker. The substrates are prepared by wiping the surface with ethanol and also nitric acid. The EPD set up must consists of steel substrate connected to the positive terminal and the U-shaped counter substrate connected to the negative terminal. Placed the steel substrate in between the U-shaped counter substrate proportionally then submerged in aqueous suspension. The procedure continues with the EPD of steel substrate with voltage deposition of 30V to 50V with the deposition time duration of 20s. Gently removed the coated samples and air dried them before sending them off for sintering process. The sintering profile are 800°C for 90 minutes with rate of increment of 2°C/min with starting temperature of 30°C.

2.3 Elemental Distribution

Energy Dispersive Spectroscopy (EDS, JSM 6380LA-JEOL, Japan) was performed to identify elemental distribution of the $(\text{MnCO})_3\text{O}_4$ spinel coated steel substrate.

2.4 Surface Morphology and Thickness

Deposition morphology and thickness were examined by Scanning Electron Microscopy (SEM) (JSM-6380LA JEOL, Japan).

2.5 Area Specific Resistance

The area specific resistance are examined by using NOVA 1.11 Autolab with each sample prepared into size of 1.0cm².

3. Results and Discussion

3.1 Elemental Distribution

Based on the results obtained from EDS shows the spinel coating contains several fixed elements. The elemental distribution for $(\text{MnCO})_3\text{O}_4$ is shown in Figure below. All the elements in $(\text{MnCO})_3\text{O}_4$ were detected in EDS.

Table 1 - Elemental distribution (MnCO)₃O₄ of composites

Elements	Atomic (%)
C	3.92
O	60.96
Si	0.18
Cr	5.45
Mn	14.15
Fe	0.98
Co	14.36
Total	100

3.2 Surface Morphology

The micrograph of (MnCO)₃O₄ spinel coating deposited at 30V, 35V, 40V, 45V and 50V are shown in Figure 1. The coating deposited on (a) 30V, (b) 35V and (e) 50V shows a non-uniform spinel deposition on which occurs because of the electrolysis of water and the poorly distributed particles [20]. Coatings on the surface of (c) 40V and (d) 45V shows a uniform deposition with denser microstructure. In order to increase homogeneity and produce uniform surface structure, higher deposition is a priority creates a more packed and dense coating structure [21], [32].

The lower the voltage deposition, the lower the particle mobility energy which contributes to the non-uniform surface coating on 30V and 35V samples. The particles possesses less energy for the particles to deposit evenly on the steel substrate. The comparatively brief period of thermal conversion and consequently incomplete interdiffusion may be associated with non-uniformity. Only insular voids, which was much lower in dimension than (MnCO)₃O₄ particles, were in the converted coating layer. This implies that Mn and Co cations' dispersal rates are very probable of the same size order in the layer [22]. When voltage deposition is too high (50V) being applied, the surface coating becomes non-uniform as the particles mobility energy becomes more energized thus faster movement of particles deposited on the steel substrate [23], [31]. As the deposition of particles on the steel is fast, the random particles arrangement does not spread widely and evenly enough as the voltage is high and the coating duration (20s) is short. High voltage may also results in turbulence in the suspension and will cause bubbles which will affect the coating surface and depositions [24], [33]. 40V and 45V gives out a more uniform coating surface as to compare to the other three samples. This is probably because the voltage deposition is sufficient for the particles to stick evenly unto the steel and to spread widely across the steel surface.

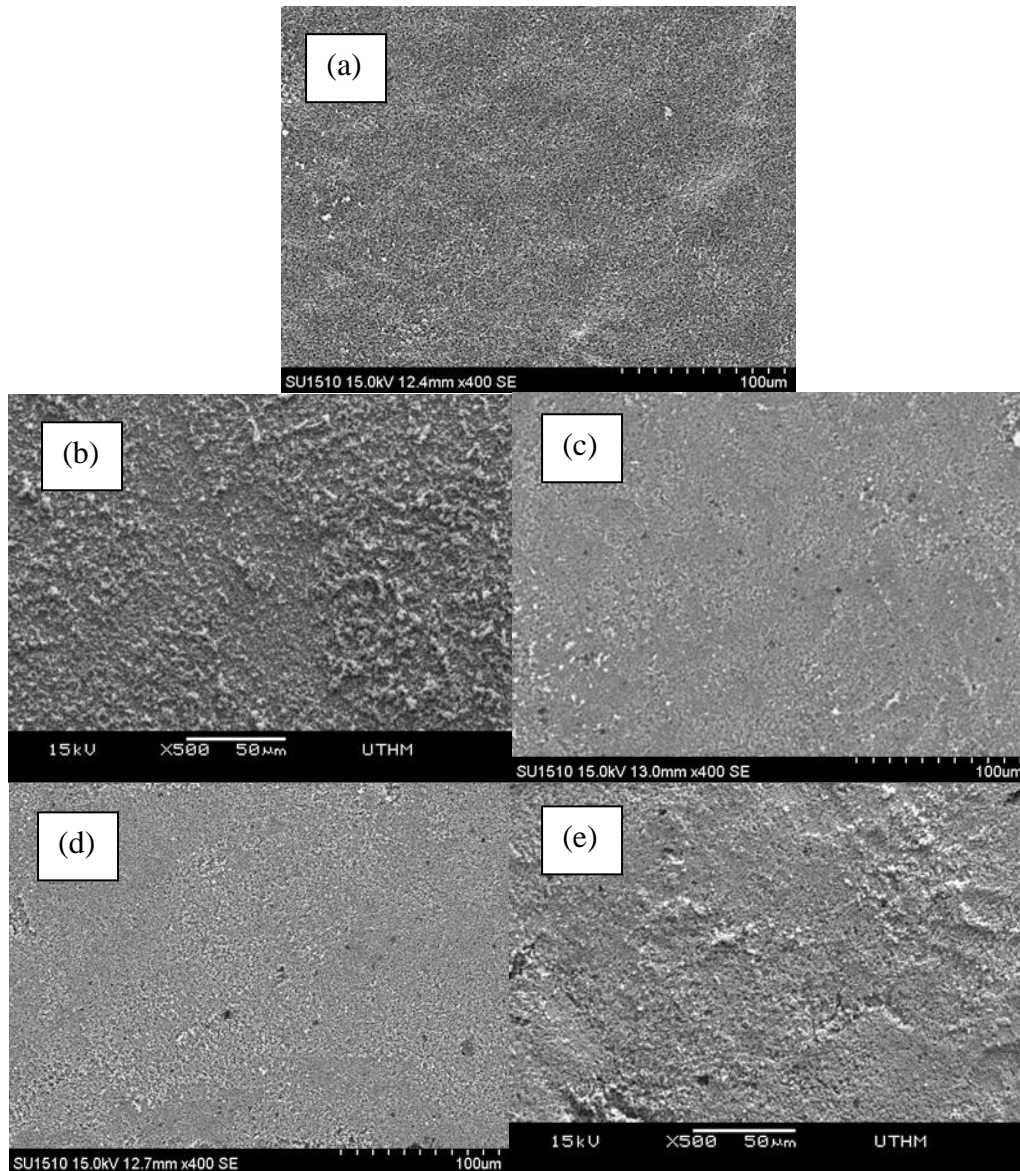


Fig. 1 - (a) 30V; (b) 35V; (c) 40V; (d) 45V; (e) 50V

3.3 Coating Thickness

The cross section of $(\text{MnCO}_3)_3\text{O}_4$ spinel coating thickness deposited at 30V, 35V, 40V, 45V and 50V are shown in Figure 2. The maximum thickness of deposition ($26.3\mu\text{m}$) of 30V was produced at 20s duration and $33.6\mu\text{m}$ maximum thickness deposition for 35V was produced for duration of 20s. It is found out that the surface morphology for 30V for 20s and 35V for 20s were non-uniform. The maximum thickness achieved for 40V for 20s was $49.1\mu\text{m}$. As for the maximum thickness ($78.8\mu\text{m}$) of 45V was produced at 20s duration. The highest voltage applied at 50V for 20s obtained a thickness deposition of $46.3\mu\text{m}$. However, the deposition thickness decrease as voltage is higher and the deposition becomes longer. By comparing between the morphology and thickness, 40V, 45V and 50V for duration of 20s produces a more homogenous, dense, better uniformity and has achieved EPD coating thickness requirement which is below $100\mu\text{m}$ [25].

At lower voltage, the coating thickness is thin and uneven. This happens because the particle mobility energy is less thus the particles in the suspension does not have enough energy to move effectively towards the steel surface. A higher voltage will contributes to a thicker coating [26] but if too high voltage is applied, coating thickness becomes lesser probably because of the high mobility energy of particles causes the particles to moves towards the steel surface at a fast rate and does not bind sufficiently [27]. This might be also be affected by the turbulence in the aqueous suspension and also the formation of bubbles in the suspension [23], [24], [31], [33].

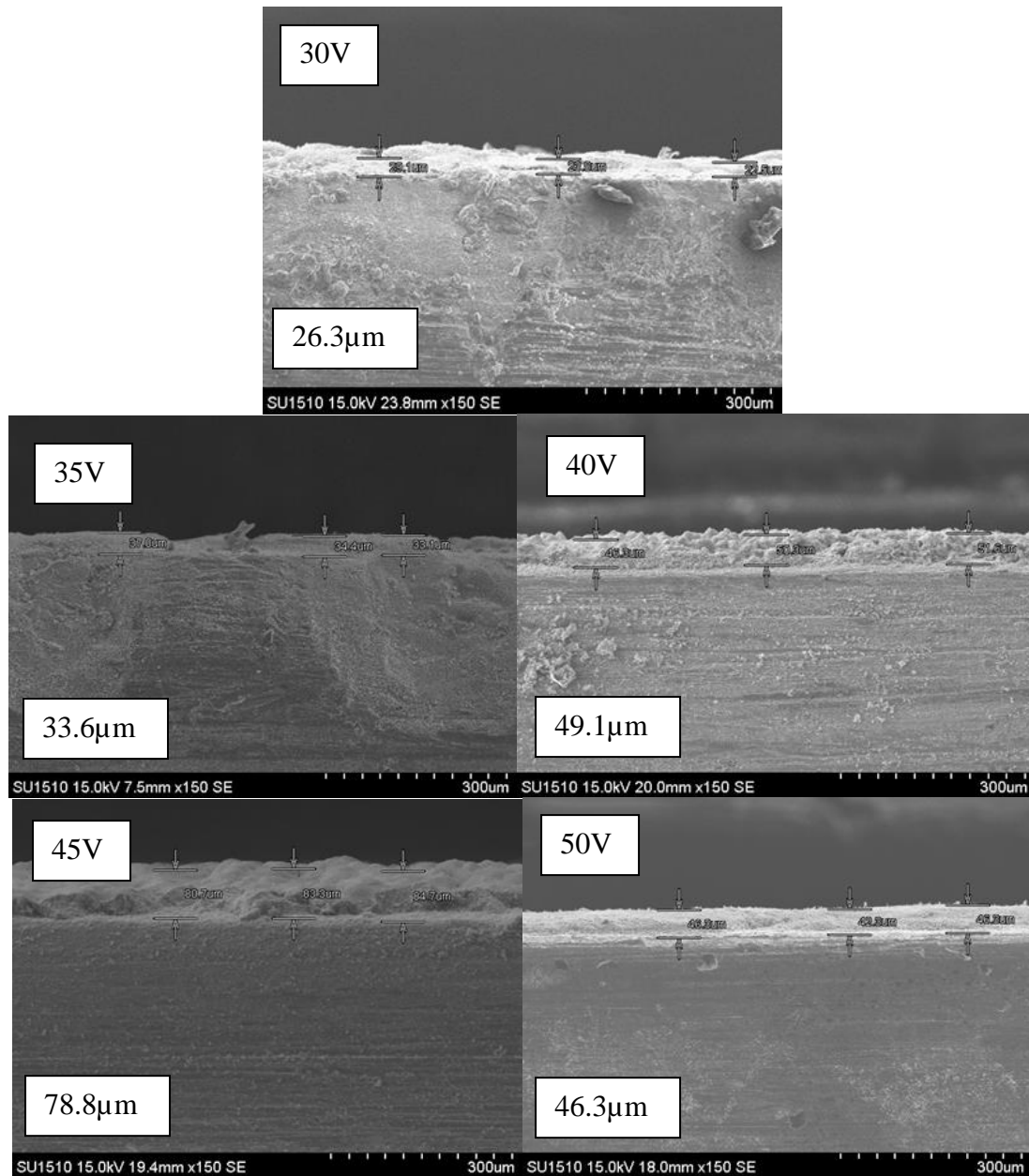


Fig. 1 - Coating Thickness for 30V, 35V, 40V, 45V and 50V

3.4 Area Specific Resistance

The $(\text{MnCO})_3\text{O}_4$ spinel coated stainless steel were tested for their electrical resistivity which is the ASR. The testing was conducted on each samples (30V, 35V, 40V, 45V and 50V) using NOVA Autolab with set temperature of 800°C with duration of 100 hours.

For 30V for 20s, the ASR reading during the beginning of testing is 0.071. As the temperature rises to 800°C , the starting ASR exceeds 0.1. After 32 hours, ASR value for 30V taken was 0.108 which is lower than the starting hour for 800°C . The ASR value for 35V at the start of testing is $0.070\Omega.\text{cm}^2$ and as soon as the temperature rises to 800°C , ASR value is $0.108\Omega.\text{cm}^2$. The starting ASR value for 40V was $0.069\Omega.\text{cm}^2$ and the ASR value at temperature 800°C for 20hr is $0.117\Omega.\text{cm}^2$. As for 40V sample, the starting ASR value is $0.069\Omega.\text{cm}^2$. At 800°C for 20 hr, the ASR value is $0.114\Omega.\text{cm}^2$. For 50V sample, reading are taken from the starting until 72hr. The starting reading for ASR is 0.164 which is very high compare to other samples. The reading then gradually lower down at the starting temperature of 800°C with ASR value of $0.120\Omega.\text{cm}^2$. After 24hr, the ASR value continues to lower to $0.105\Omega.\text{cm}^2$. ASR value then continues to lower to $0.102\Omega.\text{cm}^2$ after 72hr.

At the start of the testing, ASR value for 30V, 35V, 40V and 45V except for 50V is lower than $0.1\Omega.\text{cm}^2$. But the ASR gradually increases over time with increase in temperature except for 50V sample. But all sample exceeds the acceptable ASR value of $0.1\Omega.\text{cm}^2$ as soon as it reaches the set temperature of 800°C . The reason why the ASR value

needs to be below $0.1 \Omega \cdot \text{cm}^2$ because interconnect needs to meet specific demands which one of it is to have ASR value to be below $0.1 \Omega \cdot \text{cm}^2$ in order to achieve excellent electrical conductivity [4], [28], [29], [31]. The $(\text{MnCO})_3\text{O}_4$ spinel coating must have low ohmic resistance to maximize electrical efficiency [28], [30], [33]. Lower and acceptable ASR value also prevents chromium poisoning of the interconnects which will affect its electrical performance [21], [32].

Table 2 - ASR for $(\text{MnCO})_3\text{O}_4$ interconnects

Sample (V)	Temperature (°C)	Time (hr)	ASR ($\Omega \cdot \text{cm}^2$)
30	Starting	-	0.071
	800	Starting	0.113
	800	32	0.108
35	Starting	-	0.070
	800	Starting	0.108
40	Starting	-	0.069
	800	20	0.117
45	Starting	-	0.069
	800	20	0.114
50	Starting	-	0.164
	800	Starting	0.120
	800	24	0.105
	800	72	0.102

4. Conclusion

The spinel coated SS with deposition voltage of 30V, 35V, 40V, 45V and 50V under deposition duration of 20s were found to be not a suitable parameter for fabrication of SOFC interconnect as all did not achieved the required electrical resistance which is needed to satisfy interconnects excellent electrical conductivity besides avoiding the possibility of chromium poisoning. The most promising coating parameter for the SOFC interconnects is 40V and 45V as the surface morphology and the coating thickness satisfy the interconnect suitability demands. Based on the results, when the voltage increases, the coating thickness increases up to a certain point. Through this study, voltage deposition can be conclude to influence the performance of the steel interconnect electrical performance.

Acknowledgement

The authors gratefully acknowledges the financial support provided by H375 matching grant from Research and Innovation Fund of Research Management Centre (RMC), Universiti Tun Hussein Onn Malaysia (UTHM) and M001 contract grant from RMC, UTHM and Cellstra Sdn. Bhd..

References

- [1] Baharuddin, N. A., Muchtar, A., Somalu, M. R., Muhammed, A., & Abd Rahman, H. (2016). Influence of sintering temperature on the polarization resistance of $\text{La}_{0.6}\text{Sr}_{0.4}\text{Co}_{0.2}\text{Fe}_{0.8}\text{O}_{3-\delta}$ -SDC carbonate composite cathode. *Ceramics-Silikáty*, 60(2), 115-121
- [2] Lee, S., Chu, C. L., Tsai, M. J., & Lee, J. (2010). High temperature oxidation behavior of interconnect coated with LSCF and LSM for solid oxide fuel cell by screen printing. *Applied Surface Science*, 256(6), 1817-1824
- [3] Timurkutluk, B., Timurkutluk, C., Mat, M. D., & Kaplan, Y. (2016). A review on cell/stack designs for high performance solid oxide fuel cells. *Renewable and Sustainable Energy Reviews*, 56, 1101-1121
- [4] Fontana, S., Amendola, R., Chevalier, S., Piccardo, P., Caboche, G., Viviani, M., ... & Sennour, M. (2007). Metallic interconnects for SOFC: Characterisation of corrosion resistance and conductivity evaluation at operating temperature of differently coated alloys. *Journal of Power Sources*, 171(2), 652-662
- [5] Fergus, J. W. (2005). Metallic interconnects for solid oxide fuel cells. *Materials Science and Engineering: A*, 397(1-2), 271-283
- [6] Yang, Z., Hardy, J. S., Walker, M. S., Xia, G., Simner, S. P., & Stevenson, J. W. (2004). Structure and conductivity of thermally grown scales on ferritic Fe-Cr-Mn steel for SOFC interconnect applications. *Journal of the Electrochemical Society*, 151(11), A1825
- [7] Choi, J. J., Ryu, J., Hahn, B. D., Yoon, W. H., Lee, B. K., & Park, D. S. (2009). Dense spinel MnCo_2O_4 film coating by aerosol deposition on ferritic steel alloy for protection of chromic evaporation and low-conductivity scale formation. *Journal of materials science*, 44(3), 843-848
- [8] Liu, Y. (2008). Performance evaluation of several commercial alloys in a reducing environment. *Journal of Power Sources*, 179(1), 286-291

- [9] Kim, J. H., Song, R. H., & Hyun, S. H. (2004). Effect of slurry-coated LaSrMnO₃ on the electrical property of Fe–Cr alloy for metallic interconnect of SOFC. *Solid State Ionics*, 174(1-4), 185-191
- [10] Wu, J., Li, C., Johnson, C., & Liu, X. (2008). Evaluation of SmCo and SmCoN magnetron sputtering coatings for SOFC interconnect applications. *Journal of power sources*, 175(2), 833-840
- [11] Sun, C., Hui, R., & Roller, J. (2010). Cathode materials for solid oxide fuel cells: a review. *Journal of Solid State Electrochemistry*, 14(7), 1125-1144
- [12] Wei, W., Chen, W., & Ivey, D. G. (2009). Oxidation resistance and electrical properties of anodically electrodeposited Mn–Co oxide coatings for solid oxide fuel cell interconnect applications. *Journal of Power Sources*, 186(2), 428-434
- [13] Zhang, H., Zhan, Z., & Liu, X. (2011). Electrophoretic deposition of (Mn, Co) 3O₄ spinel coating for solid oxide fuel cell interconnects. *Journal of Power Sources*, 196(19), 8041-8047
- [14] Yang, Z., Xia, G. G., Li, X. H., & Stevenson, J. W. (2007). (Mn, Co) 3O₄ spinel coatings on ferritic stainless steels for SOFC interconnect applications. *International Journal of Hydrogen Energy*, 32(16), 3648-3654
- [15] Hua, B., Kong, Y., Lu, F., Zhang, J., Pu, J., & Li, J. (2010). The electrical property of MnCo₂O₄ and its application for SUS 430 metallic interconnect. *Chinese Science Bulletin*, 55(33), 3831-3837
- [16] Besra, L., Zha, S., & Liu, M. (2006). Preparation of NiO-YSZ/YSZ bi-layers for solid oxide fuel cells by electrophoretic deposition. *Journal of power sources*, 160(1), 207-214
- [17] Uchikoshi, T., Suzuki, T. S., Okuyama, H., Sakka, Y., & Nicholson, P. S. (2004). Electrophoretic deposition of alumina suspension in a strong magnetic field. *Journal of the European Ceramic Society*, 24(2), 225-229
- [18] Mathews, T., Rabu, N., Sellar, J. R., & Muddle, B. C. (2000). Fabrication of La_{1-x}Sr_xGa_{1-y}Mg_yO_{3-(x+y)/2} thin films by electrophoretic deposition and its conductivity measurement. *Solid State Ionics*, 128(1-4), 111-115
- [19] Sarkar, P., & Nicholson, P. S. (1996). Electrophoretic deposition (EPD): mechanisms, kinetics, and application to ceramics. *Journal of the American Ceramic Society*, 79(8), 1987-2002
- [20] Rahman, H. A., Muchtar, A. N. D. A. N. A. S. T. U. T. I., Muhamad, N. O. R. H. A. M. I. D. I., & Abdullah, H. U. D. A. (2010). Electrophoretic Deposition of La_{0.6}Sr_{0.4}Co_{0.2}Fe_{0.8}O_{3-δ} Cathode Film on Stainless Steel Substrates. In *Advanced Materials Research* (Vol. 139, pp. 145-148). Trans Tech Publications Ltd. [21] N. Shaigan, W. Qu, D. G. Ivey, and W. Chen (2010), "A review of recent progress in coatings, surface modifications and alloy developments for solid oxide fuel cell ferritic stainless steel interconnects," *J. Power Sources*, 195(6), 1529–1542
- [22] Zhu, J. H., Lewis, M. J., Du, S. W., & Li, Y. T. (2015). CeO₂-doped (Co, Mn) 3O₄ coatings for protecting solid oxide fuel cell interconnect alloys. *Thin Solid Films*, 596, 179-184
- [23] Nanda, K. K., Maisels, A., Kruis, F. E., Fissan, H., & Stappert, S. (2003). Higher surface energy of free nanoparticles. *Physical review letters*, 91(10), 106102
- [24] Besra, L., Uchikoshi, T., Suzuki, T. S., & Sakka, Y. (2008). Bubble-Free Aqueous Electrophoretic Deposition (EPD) by Pulse-Potential Application. *Journal of the American Ceramic Society*, 91(10), 3154-3159
- [25] Amrollahi, P., Krasinski, J. S., Vaidyanathan, R., Tayebi, L., & Vashaee, D. (2015). Electrophoretic deposition (EPD): Fundamentals and applications from nano- to micro-scale structures. *Handbook of Nanoelectrochemistry, Springer International Publishing Switzerland*
- [26] Abdoli, H., & Alizadeh, P. (2012). Electrophoretic deposition of (Mn, Co) 3O₄ spinel nano powder on SOFC metallic interconnects. *Materials Letters*, 80, 53-55
- [27] Azmi, M. A., Ismail, N. A. A., Rizamarhaiza, M., & Taib, H. (2016, July). Characterisation of silica derived from rice husk (Muar, Johor, Malaysia) decomposition at different temperatures. In *AIP Conference Proceedings* (Vol. 1756, No. 1, p. 020005). AIP Publishing LLC
- [28] Zhu, W. Z., & Deevi, S. C. (2003). Development of interconnect materials for solid oxide fuel cells. *Materials Science and Engineering: A*, 348(1-2), 227-243
- [29] Zhu, W. Z., & Deevi, S. C. (2003). Opportunity of metallic interconnects for solid oxide fuel cells: a status on contact resistance. *Materials Research Bulletin*, 38(6), 957-972
- [30] Rahim, P. A., Shamsudin, M. S., Nazaruddin, N. A., Azmi, M. A., Mahzan, S., Ahmad, S., & Taib, H. (2016). Corresponding Email: hariati@uthm.edu.my
- [31] Yusop, U. A., Abd.Rahman, H., & Kang Huai, T. (2019). Effect of Ag Addition on the Properties of Ba_{0.5}Sr_{0.5}Co_{0.8}Fe_{0.2}O_{3-δ}-Sm_{0.2}Ce_{0.8}O_{1.9} Composite Cathode Powder. *International Journal of Integrated Engineering*, 11(7), 169-174
- [32] Yamamoto, T., Ishimaru, K., Osman, K., Kori, M. I., Khudzari, A. Z., & Yamamoto, T. (2018). Numerical Simulation of Concentration Over-voltage in a Polymer Electrolyte Fuel Cell under Low-Hydrogen Conditions. *International Journal of Integrated Engineering*, 10(4)
- [33] Kei Hoa, N., Abd.Rahman, H., & Rao Somalu, M. (2018). Influence of Silver (Ag) Addition on the Morphological and Thermal Characteristics of NiO-SDC Carbonate Composite Anode. *International Journal of Integrated Engineering*, 10(1)